CHAPTER 5

THE VIRTUAL CROP-MODELLING SYSTEM 'VICA' SPECIFIED FOR BARLEY

P. WERNECKE, J. MÜLLER, T. DORNBUSCH, A. WERNECKE AND W. DIEPENBROCK

Institute of Agronomy and Crop Science
Martin-Luther-University of Halle-Wittenberg, Germany

Abstract. The paper presents an improved version of the **Vi**rtual **Ca**nopy model VICA (Wernecke et al. 2000), which is developed to establish a generic functional-structural plant model (FSPM; cf. Vos et al. this volume) specified for barley (*Hordeum vulgare* L.). The model core is formulated as a set of hierarchically structured objects. These objects are related to morphological and functional 'plant units' (organs). The following processes are considered: i) organ initiation, ii) organ growth and senescence, iii) photon transfer, iv) photosynthesis, v) basic features of the carbon (C), and nitrogen (N) metabolism, and vi) mass fluxes between objects. Balance equations are defined for three different substrate classes with their mobile and immobile forms: i) substrates without N, ii) substrates without C, and iii) substrates containing both C and N. This approach leads to a set of coupled nonlinear ordinary differential equations (ODEs) to describe the balance equations of the plant–soil system in terms of the above-defined substrates. On this basis, algorithms can be specified to describe plant architecture as a function of substrate masses and organ age. The extended version of VICA discussed in the present paper is capable to simulate the influence of light and nitrogen supply on the dynamics of architecture and mass. The performance of the model system is demonstrated by simulation studies. A complete parameterization of the model with experimental data is subject to further work.

INTRODUCTION

A major benefit of functional-structural plant models is to provide a sound basis for modelling the interrelations between physiological processes and morphological structures. This is achieved by coupling a structural plant model (SPM) with process-based models (PBM). The SPM defines a network of objects which are related to organs and to the complex three-dimensional (3D) structure of plants or plant stands. On this basis, it is possible to describe the interaction of plant organs with each other and with the environment. For reliable calibration of FSPMs, objects should be defined in a way such that considered processes can be experimentally analysed.

J. Vos, L.F.M. Marcelis, P.H.B. de Visser, P.C. Struik and J.B. Evers (eds.), Functional-Structural Plant Modelling in Crop Production, 53-64.

As mentioned above, the ultimate goal in developing FSPMs is to describe adequately the inherent interactions between processes controlling plant growth and formation of plant architecture. Thus, for example, it is necessary to account for the feedback resulting from the fact that plant shoot architecture affects radiation absorption and thus photosynthesis and organ growth and vice versa. The L-system-based model of Gautier et al. (2000) shows that the regulation of branch appearance and the impact of self-shading on plant morphogenesis can be described as a function of the local light environment. A recent FSPM for wheat (Evers et al. 2006) deals with the feedback resulting from mutual effects of tillering and radiative transfer. Several models include organ initiation and growth using a temperature-driven descriptive SPM based on the phyllochron / plastochron philosophy (Fournier and Andrieu 1998; Gautier et al. 2000; Evers et al. 2005; Watanabe et al. 2005). Wernecke et al. (2000) simulate the dynamics of photon transfer in a 3D plant stand combining an SPM with a photon transfer model and with a model of plant ontogenesis that describes temperature-driven plant development in terms of a phenological scale (Wernecke and Claus 1992). Drouet and Bonhomme (2004) couple a 3D model of a maize canopy with models of radiation transfer and photosynthesis to simulate the effect of N partitioning on photosynthesis. Yang and Midmore (2005) present a dynamic model of resource allocation and growth at the whole-plant level. Their model is able to simulate the competition among various shoot and root parts, but does not take into account the location and the time of appearance of new plant structures. Substrate allocation in plants in general and carbon allocation in particular has been the subject of many studies, but there is still no generally accepted theory to explain its underlying mechanisms. A partial solution is the L-PEACH model (Allen et al. 2005). This FSPM simulates the development of tree structure and solves differential equations for carbohydrate flow and allocation.

The aim of our current research is to overcome the outlined drawbacks by developing an improved FSPM system, addressing the interrelated dynamics of plant structure and functions based on coupling the SPM with PBMs describing major processes. According to our knowledge, up to now this problem has not been solved satisfactorily by existing FSPMs.

Here, the simulation tool VICA originally developed to couple geometrical and topological features of crop canopies with photon transfer, is extended: i) to compute the organ geometry as function of dry mass invested in organ formation; ii) to include processes of primary production; and iii) to describe substrate fluxes between organs. The model consists of the following components: i) an SPM representing plant organs as triangulated surface meshes; and ii) PBMs describing organ growth and senescence, photon transfer, photosynthesis, basic features of C/N metabolism and substrate fluxes between organs. The new version of VICA uses the calibrated models SAIL (Andrieu et al. 1997) and PROSPECT (Jacquemoud et al. 1996) to describe radiation transfer and LEAFC3-N (Müller et al. 2005) to compute photosynthesis. The PBM components for organ development, metabolism and partitioning are under development. Thus, we will discuss the latter models more in detail, focussing on biophysical principles used in model formulation. In this context, we have to point out that the choice of particular approaches was also ruled

by the necessity to achieve a practicable solution regarding the demands to the model calibration, to the computation time, and to the time required to implement and test the complete FSPM system.

MODELLING METHODOLOGY AND BIOPHYSICAL PRINCIPLES

Basic version of VICA

Model structure and implementation

The model core is formulated as a set of hierarchically structured objects. These objects are related to morphological and functional 'plant units' (organs). This approach leads to a set of molar balance equations (coupled non-linear ordinary differential equations) to describe the state vector Y of the plant–soil system. The initial state defined by the vector $Y_0 = Y\ (t = t_0)$ depends on the selected simulation scenario (e.g., single solitary plant or plant stands with or without soil compartment). A plant stand represented by the variable Y is located within an elementary cell with defined dimensions to realize special boundary conditions. Software toolboxes (Matlab, The MathWorks Inc., Natick, MA, USA) are used to implement the model algorithms object-oriented.

Plant architecture, attributes of elementary surfaces and organ age

The used SPM describes the surface of plant organs as a triangle mesh. Each triangle corresponds to an elementary surface, where the latter is characterized by certain additional attributes (e.g., nitrogen mass per unit surface area as input for the module that calculates photosynthesis rate). The SPM computes organ geometry from geometric input parameters dependent on organ class (e.g., leaf), organ age tau_i (normalized temperature sum after organ initiation) and organ topology (e.g., main stem, phytomer rank 2). Further, additional attributes are assigned to the computed surface elements based on inputs provided from a database or from the process-based modules of the system. The SPM is calibrated based on experimental data (not shown here). Figure 1a gives an example of a plant stand reconstructed by the SPM.

Radiation transfer and photosynthesis

Radiation transfer is computed based on interaction of photons with object surfaces accounting for their optical properties. The following algorithms are implemented: i) Monte-Carlo-Raytracing (Ross and Marshak 1991; Soler et al. 2003), and ii) the coupled PROSPECT / SAIL approach (Andrieu et al. 1997; Jacquemoud et al. 1996). These algorithms can be applied to single plants as well as to limited or unlimited canopies. For further detail see Wernecke et al. (2000). The net photosynthesis rate $R_{PN,i}$ (mol CO_2 organ^{-1} d^{-1}) of an assimilating organ i is calculated as the sum of contributions of elementary surface elements using the nitrogen-sensitive LEAFC3-N model (Müller et al. 2005; this volume) taking into account the differences in light absorption between the individual surface elements. For all other input variables (e.g., nitrogen and chlorophyll content), no variation

across organ surface was considered. R_{PN} is simulated for all assimilating organs during the entire plant ontogenesis, where an approximation is applied to leaf sheaths and ear. Figure 1b gives an example of the performance of the SPM coupled with photon transfer and photosynthesis models. The simulation shows the vertical profile of the daily C-input density (CID). Growth and maintenance respiration are calculated as described by Müller et al. (this volume). As may be seen from Figure 1b, at the bottom of the plant stand the C-input is negative since respiration losses dominate net photosynthesis at low radiation.

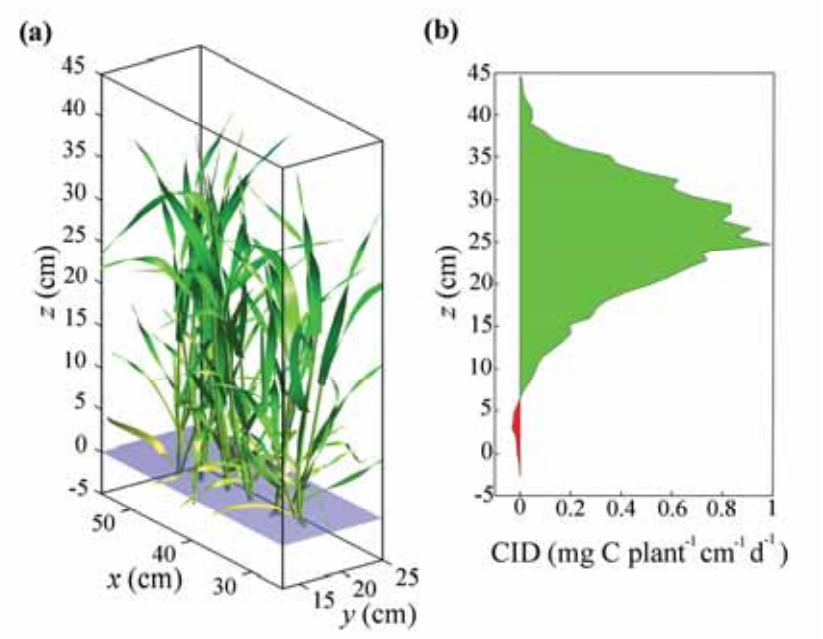

Figure 1. *(a) Spring-barley plant stand (six plants), data from field experiment (25 May 2005), 3D-visualization with the SPM. The leaf colour is coded as function of chlorophyll content (green and yellow leaves). (b) Vertical profile of carbon input density (CID)*

Model extensions: balance equations, fluxes and reaction rates

Definition of substrate classes. We define three main classes of substrates $\boldsymbol{S_k}$ (biochemical compounds, k=1...3): i) $\boldsymbol{S_1}$: $CX^{(1)}$ as a representative of C-substrates without N (e.g., saccharose, starch, cell wall components and others) to model the C-influx from photosynthesis, the transformation and transport of substrate $\boldsymbol{S_1}$; ii) $\boldsymbol{S_2}$: $NX^{(2)}$ as a representative of N-substrates without C, e.g., nitrate, to model the nitrogen uptake from the soil; and iii) $\boldsymbol{S_3}$: $C_5N_2X^{(3)}$ as a representative of C-substrates containing N, e.g., glutamine, to model the stoichiometrically coupled transport of C and N. The symbol $X^{(k)}$ refers to the components in $\boldsymbol{S_k}$ containing neither C nor N. A possible further substrate class S_4: $X^{(4)}$ is not considered. Further,

two mobility states are specified for each of these three substrate classes: the mobile state (fluxes between objects are possible, index *m*) and the immobile (fixed) state (index *f*, no fluxes are possible between objects). In the following, we introduce the molar state vectors $Y_{m,i,k}$ and $Y_{f,i,k}$ (unit: mol object^{-1}; indices: mobile(*m*) and immobile(*f*) state; object number *i*; substrate number $k = 1,2,...,n_s$; with n_s=3 substrate classes). Then the state vector *Y* of the system can be defined as:

$$Y_i = \left[Y_{m,i}\ Y_{f,i}\right]; \quad Y_{m,i} = \left[Y_{m,i,1}\ Y_{m,i,2}\ Y_{m,i,3}\right]; \quad Y_{f,i} = \left[Y_{f,i,1}\ Y_{f,i,2}\ Y_{f,i,3}\right] \tag{1}$$

If the state variable Y_i is known, the carbon mass $m_{C,i}$, the nitrogen mass $m_{N,i}$ and the dry mass m_i of organ *i* can be computed as:

$$m_{C,i} = M_C \cdot \sum_{k=1}^{n_s} \nu_{C,k} \cdot y_{i,k}\ ; \quad m_{N,i} = M_N \cdot \sum_{k=1}^{n_s} \nu_{N,k} \cdot y_{i,k}\ ; \quad m_{X,i} = \sum_{k=1}^{n_s} M_{X,k} \cdot y_{i,k} \tag{2}$$

$$m_i = m_{C,i} + m_{N,i} + m_{X,i}\ ; \quad y_{i,k} = Y_{m,i,k} + Y_{f,i,k} \tag{3}$$

M_C, M_N and $M_{X,k}$ are the molar masses of carbon, nitrogen and component $X^{(k)}$. The stoichiometric indices $\nu_{C,k}$ and $\nu_{N,k}$ are given by the structural formula of substrate $\boldsymbol{S_k}$: $C_{\nu_{C,k}} N_{\nu_{N,k}} X^{(k)}$ (e.g., $C_1N_0X^{(1)}$; $C_0N_1X^{(2)}$; $C_5N_2X^{(3)}$).

The molar-balance equations. The molar balances formulated in terms of fluxes and chemical reaction rates (cf. Bird et al. 1964; Nicolis and Prigogine 1977; Thornley 1998) define a set of coupled nonlinear ordinary differential equations (matrix notation):

$$\frac{dY_i}{dt} = B_i \cdot (R_i + \sum_j B_j \cdot F_{j \to i})\ ; \quad R_i = [R_{m,i}\ R_{f,i}]\ ; \quad F_{j \to i} = [F_{m,j \to i}\ F_{f,j \to i}] \tag{4}$$

The production term R_i [mol d^{-1}] describes the molar production rates within object *i*. The transport term $F_{i \to j}$ [mol d^{-1}] quantifies the molar fluxes between two objects (*i*, *j*). The factor B_i controls the rates R_i and fluxes $F_{i \to j}$, switches from 0 to 1, if the object is initiated (object age $tau_i > 0$).

The molar fluxes. Rearranging the equation of mass transport (Münch's hypothesis: Minchin et al. 1993; diffusion-convection equation: Bird et al. 1964), the flux $F_{m,i \to j,k}$ of the substrate $\boldsymbol{S_k}$ can be expressed as a function of the state variables (Y_i, Y_j):

$$F_{m,i \to j,k} = k_{m,i \to j,k} \cdot Y_{m,i,k} - k_{m,j \to i,k} \cdot Y_{m,j,k}\ ; \quad F_{f,i \to j,k} = 0 \tag{5}$$

$F_{m,i\rightarrow j,k}$ is defined to be positive into direction $i \rightarrow j$. For immobile components, the flux equals to zero ($F_{f,i\rightarrow j,k}$=0). The transport coefficient $k_{m,i\rightarrow j,k}$ [d^{-1}] is non-negative. Its inverse can be interpreted as characteristic transport time [d] of the substrate $\boldsymbol{S_k}$. If $k_{m,i\rightarrow j,k} = 0$ or $k_{m,j\rightarrow i,k} = 0$, the flux describes a convective transport. If $k_{m,i\rightarrow j,k} > 0$ and $k_{m,j\rightarrow i,k} > 0$, one gets a partitioning of substrates between two objects.

The production term R. We consider different types of rates *R*. The first is the net photosynthesis rate of assimilating organs $R_{PN,i}$ (computed by LEAFC3-N). Secondly, the transformation of mobile(*m*) substrate into its immobile(*f*) form is calculated as an irreversible first-order reaction (*m*—>*f*, object *i*, substrate S_k):

$$R_{f,i,k} = k_{m\rightarrow f,i,k} \cdot Y_{m,i,k} \tag{6}$$

Thirdly, we couple the C and N dynamics in leaves by a chemical reaction, which transforms the mobile substrates $\boldsymbol{S}_1$ and $\boldsymbol{S}_2$ into the reaction product $\boldsymbol{S}_3$ with a turnover rate u_i [turnovers d^{-1}]:

$$\nu_1 \cdot S_{m,i,1} + \nu_2 \cdot S_{m,i,2} \xrightarrow{u_i} \nu_3 \cdot S_{m,i,3} \tag{7}$$

$$u_i = \min\left(k_{CN,1} \cdot Y_{m,i,1},\ k_{CN,2} \cdot Y_{m,i,2}\right) \tag{8}$$

The parameters $k_{m\text{—>}f,i,k}$, $k_{CN,1}$, $k_{CN,2}$ [d^{-1}] are kinetic coefficients (Equations 6 and 8). The indices ν_k [mole $turnover^{-1}$] define the stoichiometry of the reaction (Equation 7). Then, the molar reaction rates $r_{m,i,k}$ are given by:

$$r_{m,i,1} = -\nu_1 \cdot u_i;\quad r_{m,i,2} = -\nu_2 \cdot u_i;\quad r_{m,i,3} = \nu_3 \cdot u_i;\qquad r_{m,i} = [r_{m,i,1}\ r_{m,i,2}\ r_{m,i,3}] \tag{9}$$

Fourthly, respiration losses are modelled based on the growth and maintenance concept as discussed by Müller et al. (this volume). For an organ *i*, the maintenance respiration rate *RES* is assumed to be proportional to its nitrogen mass $m_{N,i}$:

$$RES^{maint}_{m,i,1} = k_{RESm,i} \cdot (Y_{m,i,1} > 0) \cdot \max(0, m_{N,i} - N_{g,min} \cdot m_i) \tag{10}$$

This term leads to a loss of mobile (*m*) substrate S_1. The parameter $k_{RESm,i}$ is the maintenance respiration coefficient. *RES* equals zero, if there is no mobile substrate S_1 in organ *i* ($Y_{m,i,1} = 0$) or if the nitrogen mass $m_{N,i}$ is smaller than the value $N_{g,min} \cdot m_i$, where $N_{g,min}$ is a critical nitrogen content. The growth respiration rate is assumed to be proportional to the net photosynthesis rate $k_{RESg} \cdot R_{PN,i}$ (k_{RESg}: growth respiration coefficient). Using Equations 6-10, the molar production term $R_{m,i,k}$ (mobile substrates) is then given by:

$$R_{\mathrm{m,i,1}} = -R_{\mathrm{f,i,1}} + r_{\mathrm{m,i,1}} + (1 - k_{RESg}) \cdot R_{\mathrm{PN,i}} - RES^{\mathrm{maint}}_{\mathrm{m,i,1}}; \quad k > 1: \quad R_{\mathrm{m,i,k}} = -R_{\mathrm{f,i,k}} + r_{\mathrm{m,i,k}} \quad (11)$$

Mass exchange between plant and soil. We have subdivided the soil into a 3D grid and estimated the nearest grid point to the surface of a root element. The uptake rate of nitrogen and water by a root element is then computed as function of its area and of the differences in nitrogen concentration as well as in water potential between the root element and the grid point of the soil. This allows the computation of water and nitrogen uptake based on mass balance equations coupled with the water potential of leaves, which is interrelated with gas exchange (LEAFC3-N). Implemented algorithms based on the Richards and nitrate balance equation (cf. e.g., Richter 1987; Hanks 1992).

A qualitative model test

The complete model system including the extensions discussed was tested qualitatively, analysing the response of a virtual plant stand to a change in the stand density (25 and 200 plant m^{-2}, Figure 2). Tiller initiation and outgrowth according to the temporal order of tiller appearance (cf. Evers et al. 2005) is assumed to be a function of the local availability of mobile substrates $\boldsymbol{S_1}$. The light intensity at the upper boundary of the canopy was the same in both simulations, but the simulated absorbed light and carbon inputs per plant were different. Figure 2 shows the

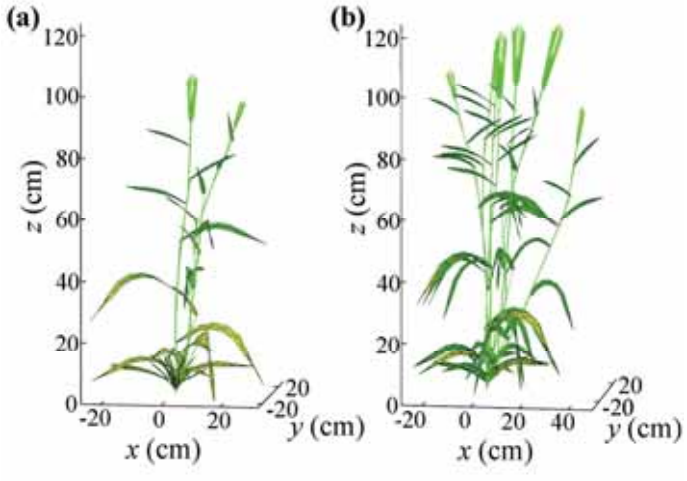

Figure 2. *Effect of light limitation on tillering. Simulated barley plant 91 days after sowing. Density of plant stand: (a) 200 plants m^{-2}, (b) 25 plants m^{-2}*

sensitivity to a change in stand density. The unknown model parameters of the molar fluxes were optimized manually. The system is capable to simulate qualitatively the effect of resource limitation (light) on tillering. To get a quantitative solution, the balance equation must be calibrated in relation to tillering in future.

MODEL APPLICATION TO C/N DYNAMICS OF BARLEY

Material and methods

Experimental setup. Spring barley (*Hordeum vulgare* L., cv. 'Barke') was chosen as model plant and analysed in a series of experiments performed under partially (glasshouse) or fully (climate chamber) controlled environmental conditions at different treatments of N supply and growth temperature. The actual environmental conditions were monitored, where average photon flux density (Q) at the top of plants in the glasshouse followed the typical seasonal pattern ($Q_{max} \approx 1000$ μmol m^{-2} s^{-1}) and approached about 400 μmol m^{-2} s^{-1} during climate-chamber experiments. CO_2 concentration ($C_a \approx 350$ ppm) and relative humidity of the air ($h \approx 70\%$) were usually maintained around specified values. Plants were grown in pots containing quartz sand with 200 mg N per plant and optimal amounts of other nutrients, avoiding any losses of N. Water was supplied to maintain soil water content of 25 volume percent. To obtain a simplified architecture of the plant (reduced number of interacting organs) that is appropriate for reliable model calibration regarding C/N balances, axillary tillers were removed twice a week.

Data base. To get a database for model calibration, the following 'objects' (organs and soil) were considered: i) leaf (visible leaf blades; rank 1 to 10), ii) stem (ensemble of nodes, internodes, leaf sheaths, folded leaf blades and invisible ear), iii) axillary tillers, iv) ear (visible part), v) root and vi) soil. Geometrical characteristics describing orientation (e.g., angles), size (e.g. length, area) and shape (e.g., surface) of organs were acquired using image processing of 2D digital images and manual measurements with a ruler or protractor. Main physiological characteristics measured were dry mass, N and C content (all organs including removed axillary tillers) and chlorophyll content (leaves), as well as light and CO_2 response curves of net photosynthesis rate (leaves). Since no geometrical information on root and stem development was available, these two objects were modelled as unstructured, whereas originally in VICA instead of *stem* several sub-objects are defined (e.g., *internode*, *node*). These objects will be specified in future based on data from our climate-chamber experiments.

Model specification and parameterization

Geometrical and optical properties of organs are calculated as a function of simulated C, N and dry mass, organ age and topology. Following characteristics of leaves are specified and parameterized based on experimental data: i) Euler angles of organ orientation, ii) area, iii) length, iv) width and v) chlorophyll content. These

characteristics are input variables to the SPM and the radiation transfer model. Regarding the architecture of organs, the following simplifications were introduced: i) *stem*: shape and elongation are described based on organ age, ii) *ear*: the number of spikelets is empirically estimated from carbon mass and organ age, and iii) *root*: architecture is not yet considered. The number of model parameters was reduced as follows: (i) we use the organ age *tau* to model the fluxes and reaction rates depending on the sequence of events (e.g., organ initiation, senescence, flowering), (ii) all leaves are modelled with the same generic parameter set (fluxes and reaction rates), and (iii) the substrate flux between two objects was modelled with maximal two parameters. If fluxes and reaction rates can be formulated as irreversible then only one parameter for a substrate flux and one for a reaction rate are sufficient. The transformation of substrates from its mobile to its immobile state (Equation 6) requires six irreversible reactions (substrates S_1, S_3 for root, stem and leaf). For nitrate reduction, one reaction is used (Equations 7-9). The following fluxes between objects $i \leftrightarrow j$ were considered (Equation 5): i) substrate S_2: soil $\rightarrow$ root $\rightarrow$stem $\rightarrow$leaf, ii) substrates S_1, S_3: leaf $\leftrightarrow$ stem, stem $\leftrightarrow$ root, stem $\rightarrow$ ear, and stem $\rightarrow$ axillary tillers. Then the total number of unknown model parameters of the specified fluxes and reaction rates is equal to 22. To estimate these parameters, the balance Equation 4 was inverted using unconstrained nonlinear optimization (Lagarias et al. 1998), minimizing the distance between simulated state vector Y and experimental data.

SIMULATION RESULTS AND DISCUSSION

To demonstrate the performance and functionality of VICA, we have above presented two examples. First, we showed in Figure 1 how our SPM works with the implemented PBMs (photon transfer, photosynthesis). The nitrogen-sensitive SPM-PBM system responds quite well to a change in vertical profiles of light, nitrogen or chlorophyll inside the canopy. In this example, all model parameters were known. In a second example, we tested our new approach to simulate the mass dynamics based on balance equations, molar fluxes and reaction rates. The results (Figure 2) show that the model is capable of simulating the outgrowth of new tillers as a result of substrate transport from leaves to tiller buds. In this example, the balance equations were not calibrated. Nevertheless, the simulation result demonstrates the possibility to model the interaction between plant organs based on fluxes and substrate transformations.

To link the dynamics of C and N, we have introduced the state vector Y defining three substrate classes. Then the carbon, nitrogen and dry mass of an organ depend on Y (Equations 2 and 3). Due to the C to N ratio of substrate $\boldsymbol{S}_3$, the C/N dynamics is coupled stoichiometrically. Therefore, the nitrogen content of organs is constrained. In the third example discussed below, we have specified and calibrated the balance equation (Equation 4) as outlined in section "*Model application to C/N dynamics of barley*". The results obtained with this model version for C/N dynamics of leaves, stem, ear, root, axillary tiller and plant are given in Figure 3. These simulations as well as those for individual leaves (not shown here) agree quite well with experimental data. The simulated mass dynamics depend on ontogenesis

events. Starting the simulation with initial condition, organs grow exponentially exchanging mass. If the ear is initiated (i.e. B_{ear} switches from zero to one, Equation 4), this new sink creates fluxes toward this new organ 'ear'. A similar pattern takes place for subsequent initiation of leaves.

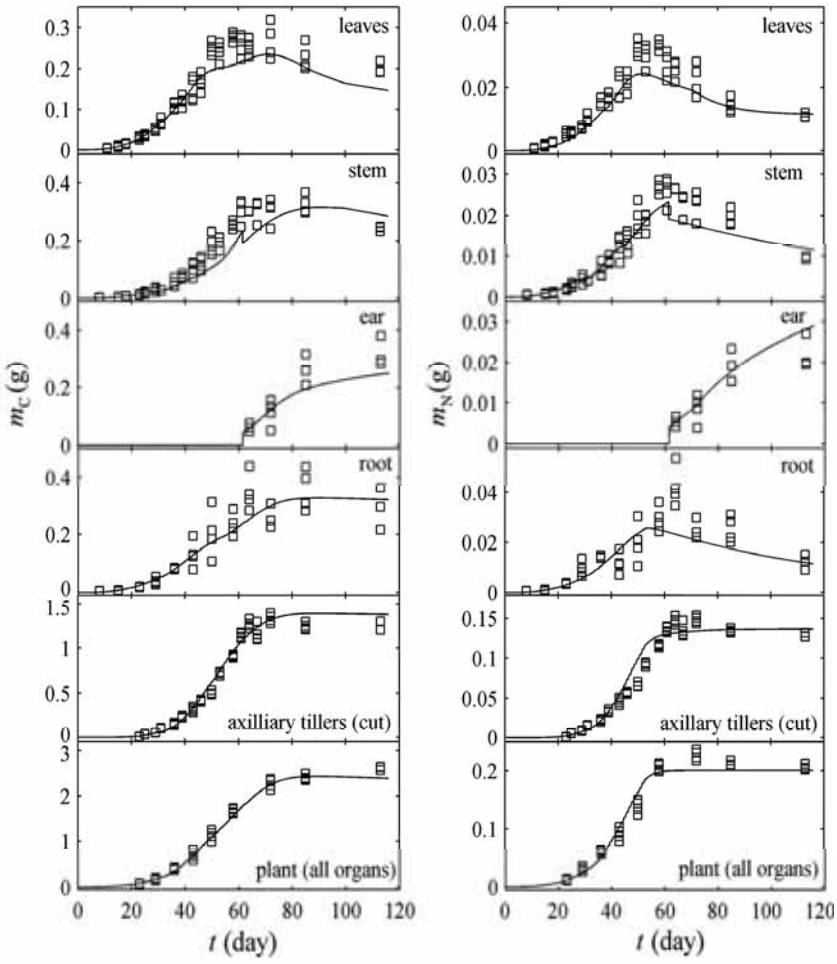

Figure 3. *Simulated time course of masses: carbon m_C (left) and nitrogen m_N (right) of leaves, stem, ear, root, axillary tillers and plant. Time t: days after sowing*

Not all of the parameter values obtained by model inversion are unique. To achieve this, additional experimental information about the substrate dynamics (fixed and mobile substrates) must be included, whereas in the current study for model inversion only the total C, total N and dry mass are used. The dependence of the model parameters on temperature is not considered. The error arising from this

assumption is rather small, since daily mean temperature in the experiments was kept nearly constant.

The simulation study shows the functionality of the virtual crop-modelling system VICA. The system combines the following main components: i) a generic SPM, ii) photon transfer and photosynthesis within the 3D plant or canopy structure, iii) source–sink-controlled allocation, and iv) transformation of substrates. This approach allows coupling the process and architecture dynamics of single plants and plant stands. In future work the model will be extended including features of the xylem / phloem transport (Yang and Midmore 2005). In general, the model system VICA can be used to model the pattern of the complex system soil – plant stand – atmosphere. The modular structure of VICA allows the implementation and test of algorithms with regard to different hierarchical levels: organ – plant – plant stand. The simulation examples presented in this paper demonstrate certain features of these capabilities.

ACKNOWLEDGEMENTS

The present study was funded by the DFG under grant DI 294/23 in the framework of the research unit ‘Virtual Crops’. The support of the state of Saxony-Anhalt is highly appreciated. Many thanks go to Dr. K. Egle and Dr. H. Beschow, Institute of Soil Science and Plant Nutrition, Martin-Luther-University of Halle-Wittenberg, who provided the carbon and nitrogen data presented in Figure 3.

REFERENCES

Allen, M.T., Prusinkiewicz, P. and DeJong, T.M., 2005. Using L-systems for modeling source-sink interactions, architecture and physiology of growing trees: the L-PEACH model. *New Phytologist*, 166 (3), 869-880.

Andrieu, B., Baret, F., Jacquemoud, S., et al., 1997. Evaluation of an improved version of SAIL model for simulating bidirectional reflectance of sugar beet canopies. *Remote Sensing of Environment*, 60 (3), 247-257.

Bird, R.B., Stewart, W.E. and Lightfoot, E.N., 1964. *Transport phenomena*. Wiley, New York.

Drouet, J.L. and Bonhomme, R., 2004. Effect of 3D nitrogen, dry mass per area and local irradiance on canopy photosynthesis within leaves of contrasted heterogeneous maize crops. *Annals of Botany*, 93 (6), 699-710.

Evers, J.B., Vos, J., Andrieu, B., et al., 2006. Cessation of tillering in spring wheat in relation to light interception and red: far-red ratio. *Annals of Botany*, 97 (4), 649-658.

Evers, J.B., Vos, J., Fournier, C., et al., 2005. Towards a generic architectural model of tillering in Gramineae, as exemplified by spring wheat (*Triticum aestivum*). *New Phytologist*, 166 (3), 801-812.

Fournier, C. and Andrieu, B., 1998. A 3D architectural and process-based model of maize development. *Annals of Botany*, 81 (2), 233-250.

Gautier, H., Měch, R., Prusinkiewicz, P., et al., 2000. 3D architectural modelling of aerial photomorphogenesis in white clover (*Trifolium repens* L.) using L-systems. *Annals of Botany*, 85 (3), 359-370.

Hanks, R.J., 1992. *Applied soil physics: soil water and temperature applications*. Springer, New York.

Jacquemoud, S., Ustin, S. L., Verdebout, J., et al., 1996. Estimating leaf biochemistry using the PROSPECT leaf optical properties model. *Remote Sensing of Environment*, 56 (3), 194-202.

Lagarias, J.C., Reeds, J.A., Wright, M.H., et al., 1998. Convergence properties of the Nelder-Mead simplex algorithm in low dimensions. *SIAM Journal on Optimization*, 9 (1), 112-147.

Minchin, P.E.H., Thorpe, M.R. and Farrar, J.F., 1993. A simple mechanistic model of phloem transport which explains sink priority. *Journal of Experimental Botany*, 44 (5), 947-955.

Müller, J., Wernecke, P. and Diepenbrock, W., 2005. LEAFC3-N: a nitrogen-sensitive extension of the CO2 and H2O gas exchange model LEAFC3 parameterised and tested for winter wheat (*Triticum aestivum* L.). *Ecological Modelling*, 183 (2/3), 183-210.]

Nicolis, G. and Prigogine, I., 1977. *Self-organization in nonequilibrium systems: from dissipative structures to order through fluctuations*. Wiley, New York.

Richter, J., 1987. *The soil as a reactor: modelling processes in the soil*. Catena, Cremlingen.

Ross, J. and Marshak, A., 1991. Monte Carlo methods. *In:* Myneni, R.B. and Ross, J. eds. *Photon-vegetation interactions: applications in optical remote sensing and plant ecology*. Springer, Berlin, 443-467.

Soler, C., Sillion, F.X., Blaise, F., et al., 2003. An efficient instantiation algorithm for simulating radiant energy transfer in plant models. *ACM Transactions on Graphics*, 22 (2), 204-233.

Thornley, J.H.M., 1998. *Grassland dynamics: an ecosystem simulation model*. CAB International, Wallingford.

Watanabe, T., Hanan, J.S., Room, P.M., et al., 2005. Rice morphogenesis and plant architecture: measurement, specification and the reconstruction of structural development by 3D architectural modelling. *Annals of Botany*, 95 (7), 1131-1143.

Wernecke, P., Buck-Sorlin, G. and Diepenbrock, W., 2000. Combining process- with architectural models: the simulation tool VICA. *Systems Analysis Modelling Simulation*, 39 (2), 235-277.

Wernecke, P. and Claus, S., 1992. Extension and improvement of descriptive models for the ontogenesis of wheat plants. *Modeling Geo-Biosphere Processes*, 1, 131-144.

Yang, Z. and Midmore, D.J., 2005. Modelling plant resource allocation and growth partitioning in response to environmental heterogeneity. *Ecological modelling*, 181 (1), 59-77.